J|A|C|S
ARTICLES
Published on Web 03/18/2006

Synthesis, Anion Exchange, and Delamination of Co−Al Layered Double Hydroxide: Assembly of the Exfoliated Nanosheet/Polyanion Composite Films and Magneto-Optical Studies

Zhaoping Liu, Renzhi Ma, Minoru Osada, Nobuo Iyi, Yasuo Ebina, Kazunori Takada, and Takayoshi Sasaki*

Contribution from the Advanced Materials Laboratory, National Institute for Materials Science (NIMS), 1-1 Namiki, Tsukuba, Ibaraki 305-0044, Japan

Received December 22, 2005; E-mail: sasaki.takayoshi@nims.go.jp

Abstract: This paper describes a systematic study on the synthesis, anion exchange, and delamination of Co−Al layered double hydroxide (LDH), with the aim of achieving fabrication and clarifying the properties of LDH nanosheet/polyanion composite films. Co−Al−CO_3 LDH hexagonal platelets of 4 μm in lateral size were synthesized by the urea method under optimized reaction conditions. The as-prepared CO_3^{2-}-LDH was converted to Cl^--LDH by treating with a NaCl−HCl mixed solution, retaining its high crystallinity and hexagonal platelike morphology. LDHs intercalated with a variety of anions (such as NO_3^-, ClO_4^-, acetate, lactate, dodecyl sulfate, and oleate) were further prepared from Cl^--LDH via an anion-exchange process employing corresponding salts. Exchanged products in various anion forms were found to show different delamination behaviors in formamide. Among them, best results were observed for NO_3^--LDH in terms of the exfoliating degree and the quality of the exfoliated nanosheets. The delamination gave a pink transparent suspension containing well-defined nanosheets with lateral sizes of up to 2 μm. The resulting nanosheets were assembled layer-by-layer with an anionic polymer, poly(sodium styrene 4-sulfonate) (PSS), onto quartz glass substrates to produce composite films. Magnetic circular dichroism (MCD) measurements revealed that the assembled multilayer films exhibited an interesting magneto-optical response.

Introduction

Layered double hydroxides (LDHs), also known as anionic or hydrotalcite-like clays, are a class of lamellar compounds that consist of positively charged brucite-like host layers and hydrated exchangeable anions located in the interlayer gallery for charge balance. The charge of the brucite-like layers arises from the isomorphous substitution of a part of the divalent metal ions with trivalent ones. The chemical composition of LDHs are expressed by the general formula $[M^{II}_{1-x}M^{III}_x(OH)_2][A^{n-}_{x/n}\cdot mH_2O]$, where M^{II} and M^{III} represent di- and trivalent metal ions within the brucite-like layers, and A^{n-} is an interlayer anion.[1]

LDHs have been the subject of intense research because of their wide applications as catalysts,[2] catalyst precursors,[3] anion exchangers,[4] acid absorbents,[5] bioactive nanocomposites,[6] electroactive and photoactive materials,[7] and so on. However, many of the applications are largely restricted due to the inaccessibility to the inner surfaces of the host layers. The most effective solution to this problem may be delamination of LDHs into single layers as this maximizes utility of the layers.[8] On the other hand, the exfoliated host layers (i.e., nanosheets), which are positively charged and have an exceedingly high two-dimensionality with a molecular thickness, may provide an ideal model system, with which we can experimentally investigate the fundamental physical properties. The nanosheets are also expected to be used as building blocks for the construction of various functional nanocomposites or nanostructures. Nevertheless, the strong electrostatic interactions between LDH layers and guest anions, which result from the high charge density of LDH layers associated with a high content of intercalated hydrated anions, make the delamination difficult. The interlayer

(1) (a) Allmann, R. *Acta Crystallogr.* **1968**, *24B*, 972. (b) Taylor, H. F. W. *Mineral. Mag.* **1973**, *39*, 377. (c) Miyata, S. *Clays. Clay Miner.* **1975**, *23*, 369. (d) Miyata, S.; Okada, A. *Clays. Clay Miner.* **1977**, *25*, 14. (e) Miyata, S. *Clays. Clay Miner.* **1983**, *31*, 305. (f) Clearfield, A. *Chem. Rev.* **1988**, *88*, 125. (g) Newman, S. P.; Jones, W. *New J. Chem.* **1998**, *22*, 105.
(2) (a) Cavani, F.; Trifirò, F.; Vaccari, A. *Catal. Today* **1991**, *11*, 173. (b) Mckenzie, A. L.; Fishel, C. T.; Davis, R. J. *J. Catal.* **1992**, *138*, 547. (c) Sels, B.; De Vos, D.; Buntinx, M.; Pierard, F.; Kirsch-De Mesmaeker, A.; Jacobs, P. *Nature* **1999**, *400*, 855.
(3) (a) Busetto, C.; Del Piero, G.; Manara, G.; Trifiro, F.; Vaccari, A. *J. Catal.* **1984**, *85*, 260. (b) Gusi, S.; Pizzoli, F.; Trifiro, F.; Vaccari, A.; Del Piero, G. *Prepr. Catal.* **1987**, 753. (c) Li, F.; Tan, Q.; Evans, D. G.; Duan, X. *Catal. Lett.* **2005**, *99*, 151.
(4) Bish, D. L. *Bull. Mineral* **1980**, *103*, 170.
(5) Pavan, P. C.; Gomes, G. D.; Valim, J. B. *Microporous Mesoporous Mater.* **1998**, *21*, 659.
(6) (a) Choy, J.-H.; Kwak, S.-Y.; Park, J.-S.; Jeong, Y.-J.; Portier, J. *J. Am. Chem. Soc.* **1999**, *121*, 1399. (b) Choy, J.-H.; Kwak, S.-Y.; Jung, Y.-J.; Park, J.-S. *Angew. Chem., Int. Ed.* **2000**, *39*, 4042. (c) Leroux, F.; Besse, J.-P. *Chem. Mater.* **2001**, *13*, 3507.
(7) (a) Kamath, P. V.; Dixit, M.; Indira, L.; Shukla, A. K.; Kumar, V. G.; Munichandraiah, N. *J. Electrochem.* Soc. **1994**, *141*, 2956. (b) Sugimoto, A.; Ishida, S.; Hanawa, K. *J. Electrochem. Soc.* **1999**, *146*, 1251. (c) Rives, V.; Ulibarri, M. A. *Coord. Chem. Rev.* **1999**, *181*, 61. (d) Sasai, R.; Shin'ya, N.; Shichi, T.; Takagi, K.; Gekko, K. *Langmuir* **1999**, *15*, 413.
(8) (a) Adachi-Pagano, M.; Forano, C.; Besse, J.-P. *Chem. Commun.* **2000**, 91. (b) Hibino, T.; Kobayashi, M. *J. Mater. Chem.* **2005**, *15*, 653.

10.1021/ja0584471 CCC: $33.50

attractions are also dependent on the affinity of anions to LDH layers. CO_3^{2-} ions are known to have a much higher affinity to LDH layers than other anions do, and thus, the delamination of CO_3^{2-}-LDHs is believed to be almost impossible. Investigation on LDH delamination began recently, and only a few works have been reported so far.[8,9] Adachi-Pagano et al. first found that LDHs modified with long-chain organic anions exhibited delamination behaviors in some nonaqueous solvents.[8a,9c−e] For example, Zn−Al LDH containing dodecyl sulfate was delaminated in butanol under refluxing conditions or in warm acryl monomers with shearing.[8a,9c] Subsequently, Hibino et al. reported that Mg−Al LDHs modified with amino acids were easily delaminated in formamide.[9a,9f] More recently, our group successfully achieved the delamination of large-sized particles of Mg−Al−NO_3 LDH into well-defined nanosheets using formamide.[9g] Wu et al. also succeeded in the delamination of Mg−Al−NO_3 LDH in formamide with ultrasonic treatment.[9h] The delamination of LDHs in formamide was observed to be instant and spontaneous and did not need any heat or refluxing. It is regarded as a very simple and effective method for the delamination of LDHs containing different anions.

As compared with Mg−Al LDH, transition metal-bearing LDHs (such as Fe−Al, Co−Al, and Ni−Al) are known to have broader technological applications due to their special catalytic, electronic, optical, and magnetic properties.[10] Therefore, it may be more desirable to obtain these LDHs in nanosheet form. Nevertheless, to obtain high-quality nanosheets which are beneficial for their applications, well-crystallized large particles of CO_3^{2-}-free LDHs need to be prepared first, as pointed out in the above-mentioned work from our group.[9g] Conventionally, CO_3^{2-}-free LDHs were prepared by constant-pH coprecipitation of the chosen M^{2+} and M^{3+} cations with alkaline solutions,[10,11] but generally the result was poorly crystalline gel-like samples. To improve the crystallinity of the products, a subsequent aging process at a high temperature or even a hydrothermal treatment were often required, but the crystallinity and homogeneity were still not satisfactory.[11] In contrast, highly crystalline LDHs (including transition metal-bearing LDHs) in CO_3^{2-} form could be obtained via a homogeneous precipitation method by the hydrolysis of urea,[12] although the optimum preparative conditions for the bulky synthesis of their uniform and large particles have not been established yet. If these well-crystallized LDHs could be converted into CO_3^{2-}-free LDHs without changing their crystallinity and particle shapes, well-defined nanosheets of transition metal-bearing LDHs would be readily available after the delamination in formamide. However, CO_3^{2-} is very difficult to be deintercalated by a normal anion-exchange manner because of this exceptionally high affinity to LDHs.[1e,13] Recently, a very effective decarbonation method based on salt−acid treatment was developed by Iyi et al., and it was found that the use of a large excess of salts and a much diluted acid was favorable for the total recovery and shape maintenance.[14] If this salt−acid anion-exchange method is applicable to any type of CO_3^{2-}-LDHs, it may be possible to prepare various types of CO_3^{2-}-free transition metal-bearing LDHs with high crystallinity.

Recently, Ogawa et al. adopted the urea method for the synthesis of Co−Al−CO_3 LDH under hydrothermal conditions.[15] The resulting particles had a platelike morphology and were several micrometers in size. However, the hydrothermal treatment induced the oxidization of Co^{2+}, which introduced Co_3O_4 as an impurity. The hydrothermal process is also inconvenient for scaling up the product. In the present work, the large-scale synthesis of uniform and large-sized hexagonal platelets of Co−Al−CO_3 LDH has been achieved through properly controlling the concentrations of $CoCl_2$, $AlCl_3$, and urea under refluxing conditions. The Co−Al−CO_3 LDH has been converted into other forms by treatment using salt−acid mixed solutions and the subsequent normal anion-exchange process. The swelling and delamination behaviors of these intercalation products with various anions in formamide have been studied. In addition, the layer-by-layer self-assembly of the exfoliated Co−Al LDH nanosheets and anionic polymers into multilayer nanocomposite films has been demonstrated, and the magneto-optical properties on the resulting films have been examined.

Experimental Section

Synthesis of Co−Al−CO_3 LDH. The synthesis was carried out in a two-neck flask (equipped with a reflux condenser) under a nitrogen flow. In a typical procedure, $CoCl_2 \cdot 6H_2O$, $AlCl_3 \cdot 6H_2O$, and urea were dissolved in 1 dm^3 of deionized water to give the final concentrations of 10, 5, and 35 mM, respectively. Then, the mixed solution was heated at the refluxing temperature (about 97 °C) under continuous magnetic stirring for 2 days. The resulting pink, solid product was filtered, washed with deionized water and anhydrous ethanol several times, and finally air-dried at room temperature.

Decarbonation and Anion Exchange of Co−Al LDH. The deintercalation of carbonate ions from the as-prepared CO_3^{2-}-LDH was carried out by treating with a salt−acid mixed solution as described in ref 14. Typically, 1.0 g of the LDH sample was dispersed into 1 dm^3 of an aqueous solution containing 1 M NaCl and 3.3 mM HCl. The vessel was sealed after purging with nitrogen gas, and then was shaken

(9) (a) Hibino, T.; Jones, W. *J. Mater. Chem.* **2001**, *11*, 1321. (b) Gardner, E.; Huntoon, K. M.; Pinnavaia, T. J. *Adv. Mater.* **2001**, *13*, 1263. (c) O'Leary, S.; O'Hare, D.; Seeley, G. *Chem. Commun.* **2002**, 1506. (d) Chen, W.; Qu, B. *Chem. Mater.* **2003**, *15*, 3208. (e) Chen, W.; Feng, L.; Qu, B. *Chem. Mater.* **2004**, *16*, 368. (f) Hibino, T. *Chem. Mater.* **2004**, *16*, 5482. (g) Li, L.; Ma, R.; Ebina, Y.; Iyi, N.; Sasaki, T. *Chem. Mater.* **2005**, *17*, 4386. (h) Wu, Q.; Olafsen, A.; Vistad, Ø. B, Roots, J.; Norby, P *J. Mater. Chem.* **2005**, *15*, 4695.

(10) For example: (a) Ehlsissen, K. T.; Delahaye-Vidal, A.; Genin, P.; Figlarz, M.; Willmann, P. *J. Mater. Chem.* **1993**, *3*, 883. (b) Xu, R.; Zeng, H. C. *Chem. Mater.* **2001**, *13*, 297. (c) Caravaggio, G. A.; Detellier, C.; Wronski, Z. *J. Mater. Chem.* **2001**, *11*, 912. (d) Jayashree, R. S.; Kamath, P. V. *J. Power Sources* **2002**, *107*, 120. (e) Segal, S. R.; Anderson, K. B., Carrado, K. A.; Marshall, C. L. *Appl. Catal. A-Gen* **2002**, *231*, 215. (f) Choudhary, V. R.; Dumbre, D. K.; Uphade, B. S.; Narkhede, V. S. *J. Mol. Catal. A: Chem.* **2004**, *215*, 129. (g) Liu, X. M.; Zhang, Y. H.; Zhang, X. G.; Fu, S. Y. *Electrochim. Acta* **2004**, *49*, 3137.

(11) For example: (a) Ulibarri, M. A.; Fernández, J. M.; Labajos, F. M.; Rives, V. *Chem. Mater.* **1991**, *3*, 626. (b) Ribet, S.; Tichit, D.; Coq, B.; Ducourant, B.; Morato, F. *J. Solid State Chem.* **1999**, *142*, 382. (c) Labajos, F. M.; Sastre, M. D.; Trujillano, R.; Rives, V. *J. Mater. Chem.* **1999**, *9*, 1033. (d) Velu, S.; Suzuki, K.; Kapoor, M. P.; Tomura, S.; Ohashi, F.; Osaki, T. *Chem. Mater.* **2000**, *12*, 719. (e) Johnson, C. A.; Glasser, F. P. *Clays Clay Miner.* **2003**, *51*, 1.(f) Li, F.; Liu, J.; Evans, D. G.; Duan, X. *Chem. Mater.* **2004**, *16*, 1597.

(12) (a) Cai, H.; Hillier, A. C.; Franklin, K. R.; Nunn, C. C.; Ward, M. D. *Scinece* **1994**, *266*, 1551. (b) Costantino, U.; Marmottini, F.; Nocchetti, M.; Vivani, R. *Eur. J. Inorg. Chem.* **1998**, *10*, 1439. (c) Costantino, U.; Coletti, N.; Nocchetti, M.; Aloisi, G. G.; Elisei, F.; Latterini, L. *Langmuir* **2000**, *16*, 10351. (d) Ogawa, M.; Kaiho, H. *Langmuir* **2002**, *18*, 4240. (e) Oh, J.-M.; Hwang, S.-H.; Choy, J.-H. *Solid State Ionics* **2002**, *151*, 285. (f) Adachi-Pagano, M.; Forano, C.; Besse, J.-P. *J. Mater. Chem.* **2003**, *13*, 1988. (g) Sileo, E. E.; Jobbagy, M.; Paiva-Santos, C. O.; Regazzoni, A. E. *J. Phys. Chem. B* **2005**, *109*, 10137.

(13) (a) Allada, R. K.; Navrotsky, A.; Berbeco, H. T.; Casey, W. H. *Science* **2002**, *296*, 721. (b) Allada, R. K.; Pless, J. D.; Nenoff, T. M.; Navrotsky, A. *Chem. Mater.* **2005**, *17*, 2455.

(14) (a) Iyi, N.; Matsumoto, T.; Kaneko, Y.; Kitamura, K. *Chem. Mater.* **2004**, *16*, 2926. (b) Iyi, N.; Matsumoto, T.; Kaneko, Y.; Kitamura, K. *Chem. Lett.* **2004**, *33*, 1122. (c) Iyi, N.; Okamoto, K.; Kaneko, Y.; Matsumoto, T. *Chem. Lett.* **2005**, *34*, 932.

(15) Kayano, M.; Ogawa, M. 48th Clay Science Conference of Japan, 2004.

for 12 h at ambient temperature. The exchanged product was isolated using the same procedure as described for the pristine material.

The LDH products with various inorganic or organic anions were prepared further by a conventional anion-exchange process using the NaCl−HCl treated LDH sample as the precursor. Typically, 0.5 g of the NaCl−HCl treated LDH sample was dispersed into 500 cm^3 of an aqueous solution containing 0.1 M sodium or potassium salts of the desired anions. The subsequent procedures were the same as those described above. Some common inorganic and organic salts as well as long-chain surfactants were used, including sodium nitrate ($NaNO_3$), sodium perchlorate ($NaClO_4$), sodium acetate (CH_3COONa), sodium lactate ($CH_3CH(OH)COONa$), sodium dodecyl sulfate ($C_{12}H_{25}OSO_3$-Na), and potassium oleate ($C_{17}H_{33}COOK$).

Exfoliation of Co−Al LDHs. The exchanged product (0.1 g) was mixed with 100 cm^3 of formamide in a conical beaker, which was tightly capped after purging with nitrogen gas. Then, the mixture was agitated vigorously in a mechanical shaker at a speed of 160 rpm for 2 days. To remove the unexfoliated particles, the resulting pink, translucent colloidal suspension was further treated by centrifugation at 2000 rpm for 10 min.

Fabrication of Multilayer Films. Multilayer ultrathin films of the exfoliated LDH nanosheets were fabricated by applying the layer-by-layer assembly procedure similar to that described previously.[9g] Substrates, such as a silicon wafer and a quartz glass slide, were cleaned by the treatment in a bath of methanol/HCl (1/1 by volume) and then concentrated H_2SO_4 for 30 min each. LDH nanosheet suspension (1.0 g dm^{-3}) obtained by delamination of NO_3^--LDH was diluted with an equal volume of Milli-Q water. First, the cleaned substrate was immersed in the diluted colloidal suspension (0.5 g dm^{-3}) of LDH nanosheets for 10 min, which was followed by rinsing with a copious amount of water. Then, the substrate treated with LDH nanosheets was dipped into a PSS aqueous solution (1.5 g dm^{-3}) for 15 min and washed with water. Subsequently, a series of deposition operations for LDH nanosheets and PSS was repeated n times to produce multilayer films of $(LDH/PSS)_n$. The resulting films were dried with a nitrogen gas flow.

Sample Characterization. The Co and Al contents of the LDH samples were determined by inductively coupled plasma (ICP) atomic emission spectroscopy (Seiko SPS1700HVR) after dissolving a weighed amount of sample with an aqueous HCl solution. The carbon content was measured on a LECO CS-444 analyzer. The water content was obtained by thermogravimetry. X-ray diffraction (XRD) data were recorded by a Rigaku Rint-2000 diffractometer equipped with graphite monochromatized Cu Kα radiation ($\lambda = 0.15405$ nm). Fourier transform infrared (FT-IR) spectra were measured on a FTS-45RD Bio-Rad infrared spectrophotometer using the KBr pellet technique in the range of 400−4000 cm^{-1}. Thermogravimetric-differential thermal analysis (TG-DTA) was carried out using a Rigaku TGA-8120 instrument in the temperature range of 25−1000 °C at a heating rate of 1 °C min^{-1} under an air flow. The morphology and dimension of the samples were examined with a JEOL JSM-6700F scanning electron microscope (SEM). Transmission electron microscopy (TEM) and selected-area electron diffraction (SAED) characterizations were performed using a JEOL JEM-3000F transmission electron microscope at an acceleration voltage of 300 kV. UV−vis absorption spectra were recorded with a Hitachi U-4100 spectrophotometer. A Seiko SPA 400 atomic force microscopy (AFM) system was used to examine the surface topography of the films deposited on Si wafers. AFM images were acquired in tapping-mode using a Si tip cantilever with a force constant of 20 N cm^{-1}. Magnetic circular dichroism (MCD) measurements (200−700 nm) at 300 K were carried out using a UV−vis MO spectrometer (Neoark BK800) with Faraday configuration in a magnetic field normal to the substrate.

Results and Discussion

Synthesis of Co−Al−CO_3 LDH. Figure 1 shows an XRD pattern of the pink product that was prepared in the $CoCl_2$−$AlCl_3$−urea system. All the diffraction peaks could be indexed as a rhombohedral structure (LDH) with the refined lattice parameters of $a = 0.30637(7)$ nm and $c = 2.2572(6)$ nm, which are consistent with those of well-known LDH materials in CO_3^{2-} form.[12] No peaks of impurities were discerned, indicating the high purity of the product. In addition, the sharp and symmetric features of the diffraction peaks strongly suggest that the produced Co−Al−CO_3 LDH was highly crystallized, having a three-dimensional order. FT-IR spectra (see Supporting Information, Figure S1) of the product provided evidence for the presence of intercalated CO_3^{2-} as well as water molecules. On the basis of the results of elemental analysis and thermogravimetric measurement (see Figure S2), the chemical composition of the obtained LDH was estimated to be $[Co_{0.67}Al_{0.33}(OH)_2][(CO_3)_{0.165}\cdot 0.49H_2O]$ (Anal. Calcd: Co, 39.1; Al, 8.8; C, 2.0; ignition loss, 31.0%. Found: Co, 38.6; Al, 8.7; C, 1.9; ignition loss, 31.3%). This composition gives a Co/Al molar ratio of 2.03 and an empirical formula weight of 101.1.

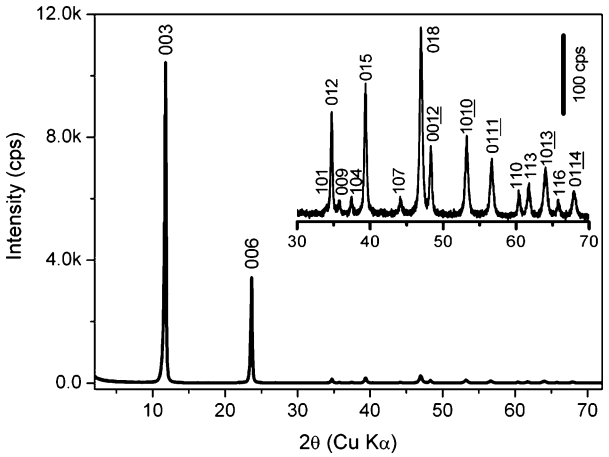

Figure 1. XRD pattern of the as-prepared Co−Al−CO_3 LDH sample. (Inset) Enlarged view of the pattern in high angles.

Figure 2 shows SEM images of a typical LDH sample. As can be seen, the sample consisted of uniform and thin hexagonal platelets with a mean lateral size as large as 4 μm and a thickness of about 30 nm. Evidently, the as-prepared Co−Al−CO_3 LDH product was of high quality in terms of morphology, size, uniformity, and crystallinity, which were much superior to those of the samples prepared by the conventional coprecipitation method. The hexagonal morphology of the particles was thought to have developed naturally as a result of the crystallographic habit (i.e., rhombohedral symmetry) of LDHs, and their uniformity, large size and high crystallinity could be attributed to a slow and homogeneous nucleation process due to the slow hydrolysis of urea. With the present synthetic parameters, the reaction could produce about 1.46 g of LDH powder, indicating a high yield rate (∼97%) compared to the expected yield (1.51 g). This powder could be readily dispersed into water or ethanol to form a colloidal suspension, as shown in the inset of Figure 2a. Similar to our recent observations on α- and β-$Co(OH)_2$ colloidal platelets,[16] the agitated platelet suspension also showed clear anisotropic streams that imply the formation of ordered structures at the macroscopic scale. This phenomenon was ascribed essentially to the anisotropic morphology and high aspect ratios of the as-prepared LDH platelets.

(16) Liu, Z.; Ma, R.; Osada, M.; Takada, K.; Sasaki, T. *J. Am. Chem. Soc.* **2005**, *127*, 13869.

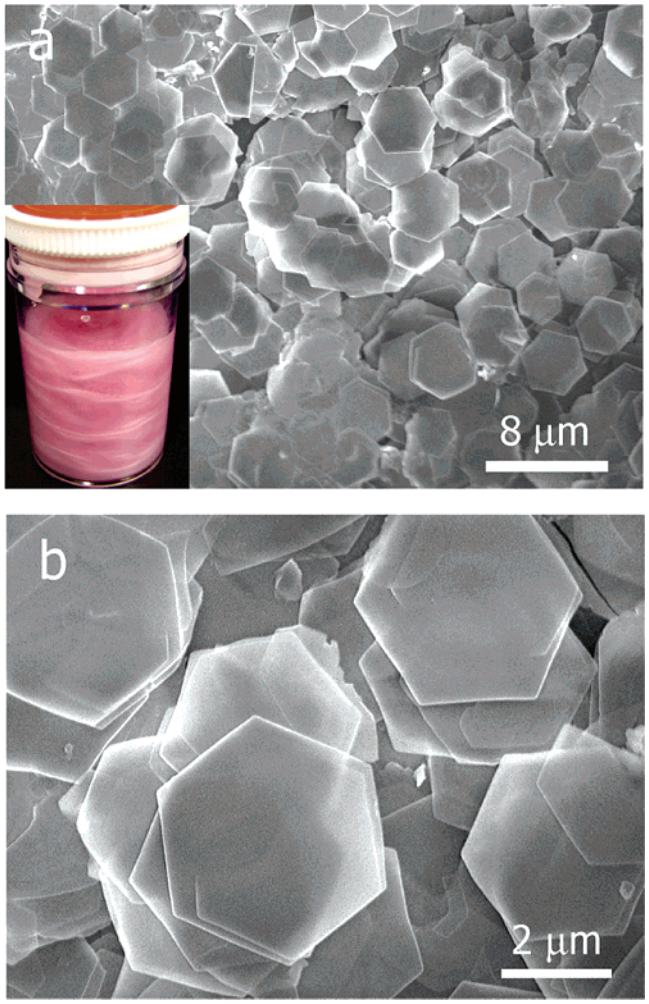

Figure 2. Low- and high-magnification SEM images of the Co−Al−CO_3 LDH sample. (Panel a inset) Bottle of LDH platelet suspension.

It has been believed that the formation of nuclei is a process that determines the final crystal sizes.[17] In general, a slow nucleation rate, which results from a low degree of supersaturation, is favorable for the growth of large crystals. For the present refluxing system, the nucleation rate could be controlled by the concentrations of total metal salts and urea. At the fixed Co/Al/urea molar ratio (2:1:7), the particle size was found to increase notably with the decreases of the total metal concentrations, as illustrated by the SEM images shown in Figure S3. For instance, the platelets prepared with 60 mM of the total metal concentration were just 1.5−2 μm in lateral sizes but had a considerable thickness of up to 80 nm. When the total metal concentration was decreased to 30 mM, the lateral sizes of the yielded platelets increased to 2−2.5 μm, but these platelets were clearly thinner (∼40 nm thick) than those prepared with 60 mM of the total metal salts. Upon decreasing the total metal concentration to 15 mM, namely the typical synthetic parameters in this paper, the platelets were about 4 μm wide and 30 nm thick, as shown in Figure 2. With a more dilute solution, the platelet size increased somewhat, but the platelets tended to have round and coarse contours, indicating that an overly low degree

(17) (a) Gilman, J. J. *The Art and Science of Growing Crystals*, Wiley: New Work, 1963. (b) Nývlt, J.; Söhnel, O.; Matuchová, M.; Broul, M. *The Kinetics of Industrial Crystallization*; Chemical Engineering Monographs, Vol. 19; Elsevier: Amsterdam, 1985.

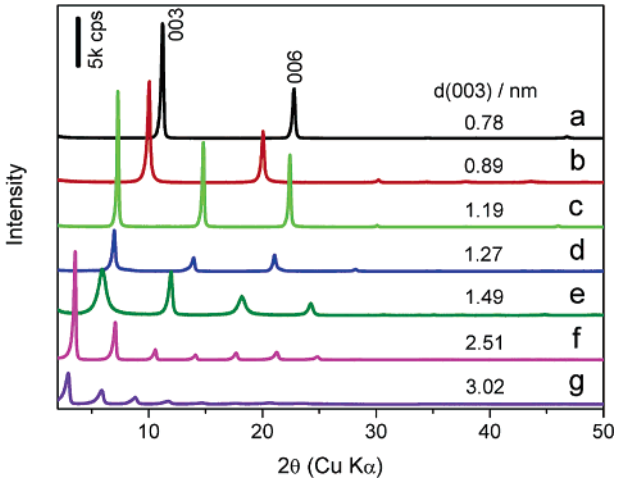

Figure 3. XRD patterns of (a) Cl^--LDH obtained by treating the CO_3^{2-}-LDH with a NaCl−HCl mixed solution, (b) NO_3^--, (c) ClO_4^--, (d) acetate-, (e) lactate-, (f) dodecyl sulfate-, and (g) oleate-LDHs prepared by treating 0.5 g of the Cl^--LDH with 500 cm^3 of aqueous solution containing 0.1 M corresponding salts.

of supersaturation was unfavorable for the growth of well-developed crystallites. On the other hand, the increase of urea concentration also led to the formation of smaller platelets; when a large excess of urea was used, the platelet size would decrease notably. For example, a mixed solution containing 15 mM of total metal salts and 0.3 M of urea yielded platelets with an average lateral size of <2 μm (see Figure S4). These results indicate that the synthetic parameters for the typical synthesis may be optimum for the preparation of uniform and large-sized Co−Al−CO_3 LDH hexagonal platelets.

Decarbonation and Anion Exchange of Co−Al LDH. The decarbonation of the as-prepared Co−Al−CO_3 LDH sample was conducted using a salt−acid mixed solution according to the method reported by Iyi et al.[14] In the present experiment, 1.0 g of CO_3^{2-}-LDH was used versus 1 dm^3 of 1 M NaCl and 3.3 mM HCl. Figure 3a shows the XRD pattern of the sample obtained by this salt−acid treatment. In this pattern, the basal reflections with d values of 0.75 and 0.375 nm (003 and 006 reflections, respectively) for the CO_3^{2-} form completely disappeared, and thereby new series of intense basal reflections at lower 2θ angles appeared instead, suggesting that the decarbonation was successful and that highly crystalline Cl^--LDH product formed. Owing to the incorporation of Cl^-, the basal spacing of the LDH increased from 0.75 to 0.78 nm. The interlayer expansion is consistent with that in previous work.[14] The complete removal of CO_3^{2-} was evidenced by the FT-IR spectrum (Figure S5a). Elemental analyses revealed that the Co/Al molar ratio of the Cl^--LDH sample was about 1.95, which was slightly less than that (2.03) of the starting CO_3^{2-}-LDH. In combination with the result of TG measurement (see Figure S5b), the chemical formula of the Cl^--LDH was determined as $[Co_{0.66}Al_{0.34}(OH)_2][Cl_{0.34}\cdot 0.46H_2O]$. SEM observations (see Figure S6) revealed that the obtained Cl^--LDH sample exhibited almost the same morphology and size as those of the starting material, suggesting that no acid corrosion took place. In addition, the weight recovery (1.0 g) was very close to the theoretical one (1.01 g) based on the estimated formula, indicative of a negligible weight loss. The quantitative weight recovery should be attributed to the usage of much dilute HCl (3.3 mM). In the current reaction system, the molar ratio of

H^+/CO_3^{2-} was calculated to be about 2.0. This value, in principle, would not induce any acid damage.[14] It should be mentioned that the acid concentration adopted in the NaCl−HCl mixed solution was found to be the least one required for achieving the complete decarbonation even though a more concentrated NaCl solution (>1 M) was used. This observation implied that Co−Al−CO_3 LDH was more difficult to be decarbonated than the Mg−Al analogue, for which a H^+/CO_3^{2-} ratio of 1.6 was enough.[14]

The above results clearly revealed that well-crystallized Co−Al−Cl LDH could be obtained conveniently from the as-prepared Co−Al−CO_3 LDH through such a simple salt−acid treatment without any morphological changes. As pointed out by Iyi,[14] the decarbonation of LDHs could also be performed with other salt−acid systems, such as $NaNO_3$−HCl and $NaClO_4$−HCl, and LDHs in NO_3^- or ClO_4^- forms would be produced directly. Nevertheless, higher acid concentrations were needed for complete decarbonation due to their relatively lower affinity for LDH in comparison with Cl^-. In these cases, the molar ratios of H^+/CO_3^{2-} exceeding 2 were required essentially in the reaction solutions. Due to the presence of an excess of protons, the dissolution of LDH layers would take place, leading to morphological change and weight loss. Therefore, Co−Al LDHs in these anion forms were preferably prepared from the as-obtained Cl^--LDH via a normal anion-exchange process since Cl^--LDH possessed high anion-exchangeability. XRD (Figure 3b and c) and FT-IR characterizations (Figure S7a and b) revealed that the complete exchange could be achieved as long as the molar amount of NO_3^- or ClO_4^- reached 20 times that of the Cl^- in the LDH. After anion exchange, the interlayer spacings of LDHs increased to 0.89 nm (for NO_3^-) and 1.19 nm (for ClO_4^-), respectively. SEM images (Figure S8a and b) showed that the obtained NO_3^-- and ClO_4^--LDH samples had the same morphology as the precursor Cl^--LDH. Furthermore, it was also found that well-crystallized LDHs containing a variety of organic anions (such as acetate, lactate, dodecyl sulfate, and oleate) could be prepared through such a simple procedure, as evidenced by the XRD patterns (Figure 3d−g) and FT-IR spectra (Figure S7c−f). After intercalating with acetate, lactate, dodecyl sulfate, and oleate anions, the interlayer spacings were expanded to 1.27, 1.49, 2.51, and 3.02 nm, respectively. In accordance, a pronounced increase of platelet thickness in proportion to the expansion of basal spacing was also observed (see Figure S8c−f).

Swelling and Exfoliation Behaviors of the Exchanged Co−Al LDHs. Through treating the as-prepared Co−Al−NO_3 LDH hexagonal platelets of 4 μm size with formamide, a pink, transparent colloidal solution (see Figure 4a) was yielded, suggesting the occurrence of delamination. A clear Tyndall light scattering was observed, indicating the presence of exfoliated LDH layers (nanosheets) dispersed in the formamide. The resulting colloidal suspension was very stable, and no sediment was observed upon long-term standing. By centrifugation at a speed of 30 000 rpm for 30 min, a pink, glue-like aggregate was recovered from the suspension. The XRD pattern of the wet colloidal aggregate is depicted in Figure 4b. The sharp basal reflections of the parent NO_3^--LDH were absent in this pattern, indicating that the layer structure had collapsed. Instead, a noticeable amorphous-like halo was observed in the low angular region (2θ, <15°). This feature can be ascribed to the scattering

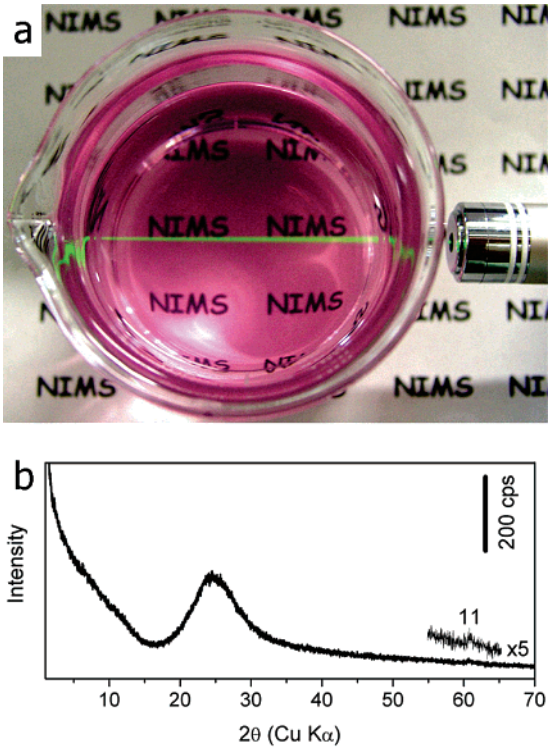

Figure 4. (a) Photograph of a colloidal suspension of exfoliated Co−Al LDH nanosheets. The light beam was incident from the side to demonstrate the Tyndall effect. The LDH content was 1.0 g dm^{-3}. (b) XRD pattern for the colloidal aggregate centrifuged from the suspension.

from a random aggregate of exfoliated nanosheets.[18] A similar broad hump has been observed for the exfoliated Mg−Al LDH nanosheets.[9g] Another feature of the halo pattern in the 2θ range of 20−30° is due to the scattering of liquid formamide.[9g] Besides these broad characters, a very faint reflection at 60.5° in 2θ was discerned, which can be assigned to 11 for a hexagonal two-dimensional unit cell with $a = 3.06$ Å. This result indicates that the two-dimensional crystalline order of the LDH layers was preserved even in the colloidal form.

The morphology and size of the exfoliated nanosheets were examined by AFM and TEM. A tapping-mode AFM image (Figure 5a) showed two-dimensional ultrathin sheets with lateral dimensions of up to 1 μm, although fragments were also observed in small amounts. Some large nanosheets with lateral dimensions of >2 μm were occasionally encountered. The exfoliated nanosheets were morphologically irregular and dimensionally diminished in comparison with the parent LDH crystallites, indicating the breakage or fracture of sheets during the delamination process. The height profile revealed that the nanosheets had a fairly flat terrace with an average thickness of 0.80 ± 0.01 nm. This value was very similar to that previously observed for Mg−Al LDH nanosheets, which has been explained as the sum of crystallographic thickness (0.48 nm) of the LDH layer and an adsorbed monolayer (~0.3 nm) of formamide molecules.[9g] Such a thickness unambiguously indicated the unilamellar nature of the delaminated nanosheets. A typical TEM image (Figure 5b) shows thin sheetlike objects with similar lateral dimensions as those detected by AFM observations. The sheets had very faint but homogeneous contrast, reflecting their ultrathin nature and uniform thickness.

(18) Sasaki, T.; Watanabe, M. *J. Am. Chem. Soc.* **1998**, *120*, 4682.

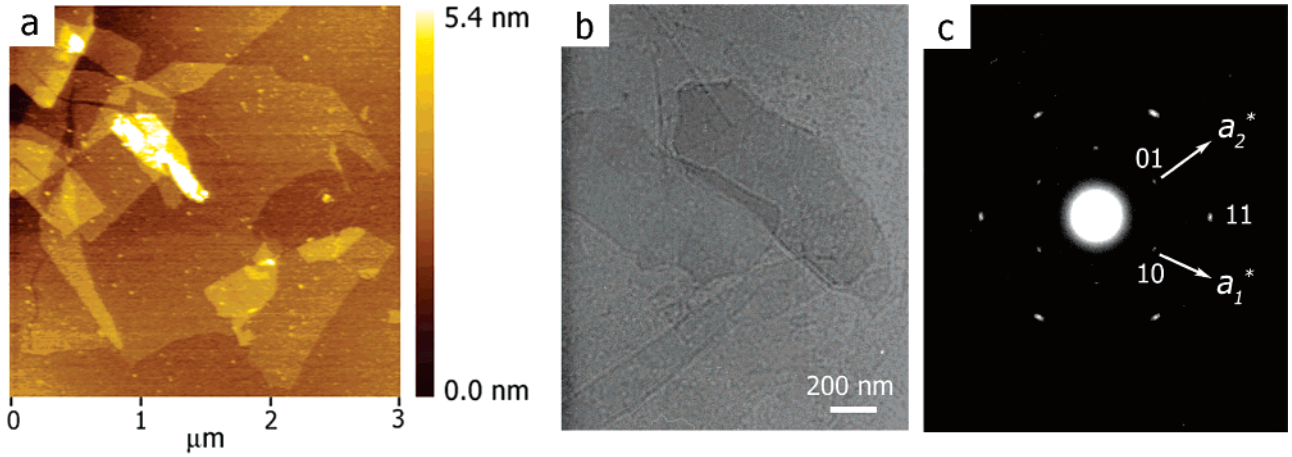

Figure 5. (a) Tapping-mode AFM image of the exfoliated LDH nanosheets deposited on a Si wafer substrate. (b) TEM image and (c) SAED pattern of LDH nanosheets.

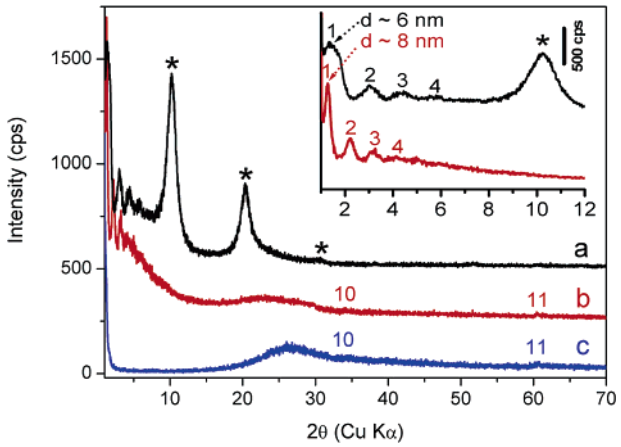

Figure 6. XRD patterns of gel-like samples obtained by mixing 0.1 g of Co−Al−NO_3 LDH powder with different volumes of formamide: (a) 0.25, (b) 0.5, and (c) 0.75 cm^3. (Insets) Enlarged view of patterns a and b in the low angular region. The peaks marked by asterisk indicate the basal reflection series related to the starting Co−Al−NO_3 LDH. The numeral at each peak shown in the inset designates the order of basal reflections for the swollen phases.

The SAED pattern (Figure 5c) of individual sheets exhibited hexagonally arranged spots, confirming their single-crystal nature. The hexagonal lattice with $a = 3.06$ Å was compatible with the in-plane structural parameter of Co−Al LDH precursor crystals determined from the XRD characterization, indicating that the basic architecture of the layer remained unchanged after exfoliation.

The delamination of LDH in formamide was observed to be very rapid, and it has been assumed that the introduction of a large volume of formamide into the interlayer space considerably weakens the interlayer attraction and thus causes the LDH sheets to come apart.[9a,f] However, there is still no detailed information on how the formamide separates the LDHs into single sheets. To understand the delamination process, it is essential to clarify what reactions have taken place between formamide and LDH crystals. For this purpose, 0.1 g of Co−Al−NO_3 LDH powders was mixed with formamide at various volumes, and the resultant viscous gels were subjected to XRD measurement. The XRD pattern (Figure 6a) of the sample in 0.25 cm^3 of formamide showed basal diffraction series in a very low angular range. The gallery height was estimated to be about 6 nm, which was largely expanded from the original value of 0.89 nm for Co−Al−NO_3 LDH. This high degree of interlayer expansion should be due to the introduction of a large volume of formamide molecules into the interlayer space, which may be comparable to "osmotic swelling" that has been observed for smectite clay minerals in water,[19] and layered titanate and manganese oxide in aqueous solution of quaternary ammonium ions.[18,20] In addition, the basal reflections of Co−Al−NO_3 LDH, despite with a much decreased intensity, were still recognized, indicating the presence of a small amount of unswollen LDH particles. When the formamide amount was increased to 0.5 cm^3, all the Co−Al−NO_3 LDH particles were swollen, and the peaks of the swollen phase shifted to lower angles (see Figure 6b), indicating that the degree of swelling was enhanced. In this case, the interlayer spacing increased to 8 nm. Upon increasing the formamide amount to 0.75 cm^3, no basal diffraction series were observed in the low angular range (>1°), and the diffraction halo in the 2θ region of 1−10° characteristic of exfoliation was not yet discerned (see Figure 6c). Such diffraction features indicated that a swollen phase with a very large gallery height (possibly up to tens of nanometers) might have formed. SEM observations (see Figure S9a and b) revealed that this sample in the microscope consisted of wrinkled hexagonal platelets having lateral size and thickness similar to those of the original particles. The well-retained morphology and size strongly suggested that only a swelling event had occurred on these platelets. The thickness recovery and wrinkles were caused by swelling collapse due to the evacuation of formamide under the superhigh vacuum condition during the SEM observations. More interestingly, Co−Al−NO_3 LDH with the same morphology, size, and crystallinity as those of the original crystals could be restored instantly from the gel upon treating with copious water, as depicted by the SEM images (Figure S9c and d) and XRD pattern (Figure S10). Such an instant and reversible conversion implied that the H-bonds between water molecules and LDH layers were much stronger than those between formamide molecules and LDH layers. In addition, the absolute restoration of the particle morphology and crystallinity implied that the swollen structure was not turbostratic but long-range-

(19) (a) Norrish, K. *Discuss. Faraday Soc.* **1954**, *18*, 120. (b) MacEwan, D. M. C.; Wilson, M. J. In *Crystal Structures of Clay Minerals and Their X-ray Identification*; Brindley, G. W., Brown, G., Eds.; Mineralogical Society: London, 1980.
(20) (a) Sasaki, T.; Watanabe, M.; Hashizume, H.; Yamada, H.; Nakazawa, H. *J. Am. Chem. Soc.* **1996**, *118*, 8329. (b) Omomo, Y.; Sasaki, T.; Wang, L. Z.; Watanabe, M. *J. Am. Chem. Soc.* **2003**, *125*, 3568.

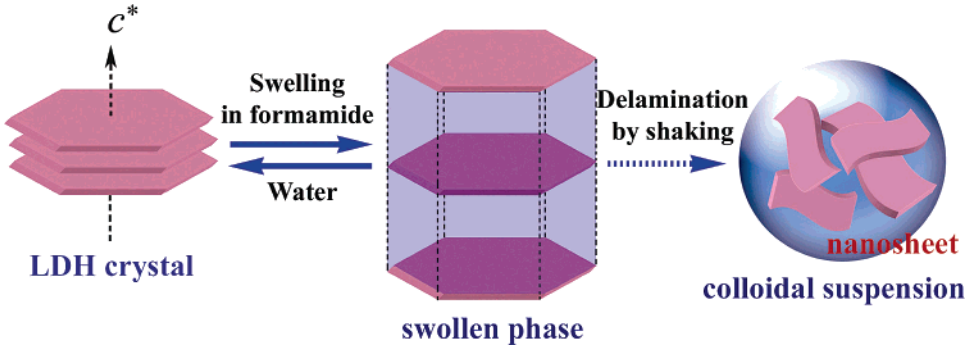

Figure 7. Schematic illustration of the possible delamination mechanism for LDHs in formamide.

ordered with a large volume of formamide in the interlayer galleries. The resulting swollen structure might be maintained by the weak H-bonding between formamide and LDH layers as well as the electrostatic attraction between layers and the guest anions. Only with the assistance of mechanical shearing or ultrasonic waves, could the swelling proceed successfully to exfoliation. In fact, our exfoliation experiment was performed with continuous and vigorous shaking, and it typically took about 2 days to achieve the complete exfoliation. Once the exfoliation had been reached, the final suspension did not return to the swollen phase. On the basis of the above results, it can be safely concluded that the delamination of LDH follows two separate processes: rapid swelling and subsequent slow exfoliation, which are depicted schematically in Figure 7. The swelling is performed instantly, and the exfoliation of the highly swollen phase proceeds progressively with the assistance of continuous shaking. This delamination process is very similar to those that have been observed for layered titanates and manganese oxide.[18,20] Thus, this mechanism should commonly exist in other layered systems. In addition, the exfoliation degrees at different stages could be determined by the separation of the unexfoliated swollen particles via centrifugation at 2000 rpm. Since the unexfoliated swollen particles could be recovered as the original LDH crystals by treating with water, the exfoliation degree of the sample could be quantitatively figured out according to the amount of recovered crystals. In particular, the exfoliating degrees after being shaken for 12 and 24 h were estimated to be about 40% and 70%, respectively, verifying the delamination was indeed a slow but progressive process.

In addition to the NO_3^--LDH, other LDHs with various intercalated anions (except for lactate and oleate) prepared in the present studies were also found to show the swelling and exfoliation behaviors in formamide, but they exhibited different degrees of exfoliation at a given time. After being shaken for 2 days, the exfoliating degrees for Cl^--, ClO_4^--, acetate-, and dodecyl sulfate-LDHs were measured to be about 75, 50, 60, and 95%, respectively. This means that the interlayer anions had great effects on the exfoliation behaviors of LDHs. For these LDHs, longer shaking periods were required to attain complete exfoliation. The nanosheets exfoliated from the LDHs intercalated with small anions (e.g., Cl^-, ClO_4^-, and acetate) displayed lateral sizes ranging from hundreds of nanometers to micrometer scale (see Figure S11a−c), which were similar to that of the nanosheets derived from the NO_3^--LDH. In contrast, the exfoliation of dodecyl sulfate-LDH yielded 20−100 nm-sized sheets (see Figure S11d), indicative of severe fracture of nanosheets.

Multilayer Composite Films of LDH Nanosheets and PSS: Layer-by-Layer Assembly and Magneto-Optical Study. In the previous report of our group,[9g] the substrates (Si wafer or quartz glass) were primed with a PEI/PSS bilayer in advance, to promote adsorption of a dense monolayer of Mg−Al LDH nanosheets. Since the substrates treated with concentrated H_2SO_4 have a negatively charged surface, the positively charged LDH nanosheets may be adsorbed spontaneously onto the substrate surface. As expected, the Si wafer substrate surface was densely tiled with LDH nanosheets (see Figure 5a), indicating that precoating a PEI/PSS bilayer was not essential. The monolayer coverage was predominant although there were some overlaps and uncovered gaps. The overall coverage was determined to be about 70%, and the overlap percentage was about 25%. It was found that, when the suspension was diluted with certain amount of water, an increased coverage could be attained. The reason may be that the positive-charged nanosheets exhibit a higher ionicity in an aqueous solution. Thus, a water-diluted suspension was preferred for film assembly. However, the addition of water into the suspension may induce flocculation upon long-period standing; the water-diluted suspension used for multilayer assembly was required to change every 12 h.

Multilayer films were obtained by alternately dipping a quartz glass slide into a colloidal suspension of the LDH nanosheets and a PSS solution. The growth of LDH/PSS multilayer films under the optimized conditions was monitored by UV−vis absorption spectra measured immediately after each deposition cycle (Figure 8). The absorption band around 200 nm is characteristic of PSS, and its nearly linear increment as a function of the number of deposition cycles indicates a stepwise and regular film growth. After the deposition of 10 bilayers, the absorbance at 193 nm was 0.34, which was comparable to that for the $(Mg-Al\ LDH\ nanosheets/PSS)_{10}$ film. When 50 bilayers were deposited, nevertheless, the absorbance at 193 nm reached 2.1 (see Figure S12), which was larger than the expected value (1.7) for the ideal film. The gradually increased roughness of the surface for the thicker film may be responsible for this behavior.

XRD patterns (Figure 9) of the multilayer films illustrate the evolution of a Bragg peak at 4.4° in 2θ, which is attributable to a so-called superlattice reflection of the inorganic/organic-repeating nanostructure. A periodicity of 2.0 nm was consistent with that observed for $(Mg-Al\ LDH\ nanosheets/PSS)_n$ films. The peak intensity increased progressively with the increase of the number of layer pairs, further verifying the successful multilayer buildup. Allowing for a thickness of about 0.48 nm

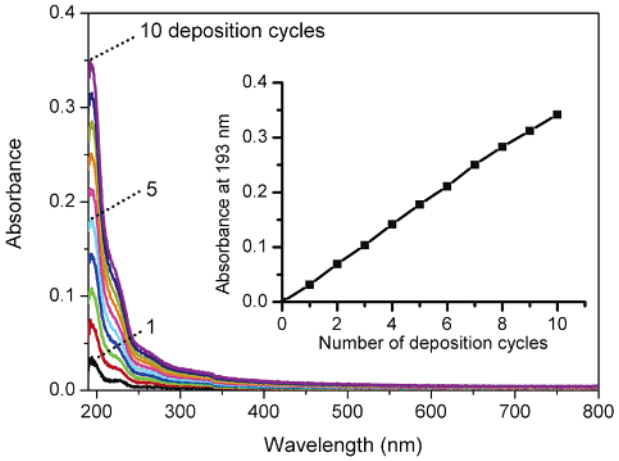

Figure 8. UV−vis absorption spectra of multilayer film of $(LDH/PSS)_n$ assembled on a quartz glass substrate. Nanosheet concentration was 0.5 g dm^{-3}; PSS concentration was 1.5 g dm^{-3}; deposition periods in nanosheet suspension and PSS solution were 10 and 15 min, respectively. The observed absorbance at 193 nm is plotted against the number of deposition cycles in the inset.

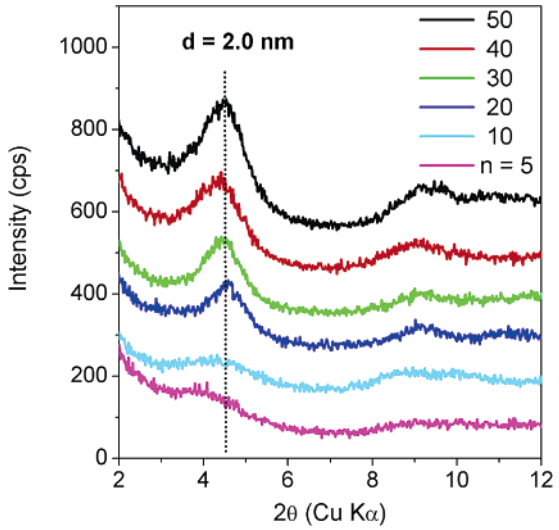

Figure 9. XRD patterns of the multilayer films of $(LDH/PSS)_n$ assembled on a quartz glass slide.

for the LDH nanosheets, the layer height of PSS along the film normal is estimated to be about 1.5 nm.

Such multilayer films constructed with two-dimensional (2D) nanosheets are of intrinsic fundamental interest since magnetic properties in 2D systems are expected to be substantially different from those in 3D bulk systems.[21] Indeed, our group found that multilayer assemblies of Cobalt-substituted titania nanosheets exhibited robust magneto-optical response at short wavelengths.[22] Since the present LDH nanosheets are Co^{2+} bearing, a ferromagnetic property may be expected. In fact, first-principle calculation on 3d transition metal LDH nanosheets predicted both ferromagnetic and half-metal states. The magneto-

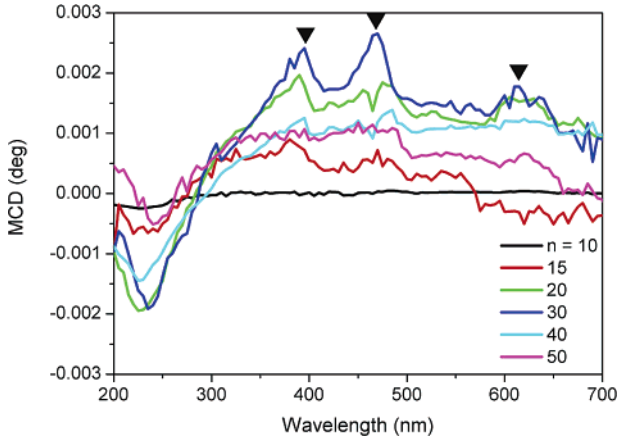

Figure 10. MCD spectra for the multilayer films of $(LDH/PSS)_n$ (n = 10, 15, 20, 30, 40, and 50) measured in 10 kOe at 300 K.

optical effects of the multilayer films of Co−Al LDH nanosheets were investigated with MCD spectroscopy, which is very useful for probing the magnetic properties of ultrathin films because the contribution from the substrate on the spectrum is negligible compared to the magnetization measurements.[22] The room-temperature MCD spectra of the as-assembled multilayer films are shown in Figure 10. It can be seen that these multilayer films with larger stacking layer numbers (n > 10) exhibited notable positive magneto-optical signals at wavelengths of >300 nm. The magnetic field dependence of the MCD signal clearly showed the ferromagnetic behavior of the nanocomposite films at room temperature. As the PSS does not show any prominent absorption in this spectral range, we conclude that the observed MCD feature was caused by Co−Al LDH nanosheets. The ferromagnetic effect of the LDH layers can be ascribed to the spin−orbit coupling in Co^{2+} in octahedral geometry. As indicated in Figure 10, three positive peaks are commonly observed in all the spectra. The MCD signal at 390 nm may be attributed to the charge transition of O2p to Co π*, and the peaks at 470 and 615 nm fall close to the d−d* transition ($A_{2g} \rightarrow T_{2g}$ and $A_{2g} \rightarrow T_{1g}$, respectively) of Co−Co. Another notable feature of these spectra was that the MCD signal was enhanced significantly as the layer stacking was increased in the first 30 layers. The dramatic increment of MCD signal with increasing number of LDH layers indicates strong interlayer couplings between the electronically isolated LDH layers. We also noted that the MCD signal reached the maximum at a layer number of 30 and further increasing the layer stacking led to a reduced response. Although further understanding of the thickness dependence awaits detailed experimental and theoretical studies, these results should stimulate extensive research on Co−Al LDH nanosheets as an important testing ground for 2D ferromagnetism.

Conclusion

In summary, we have succeeded in synthesizing uniform and large-sized hexagonal platelets of Co−Al−CO_3 LDH via a homogeneous precipitation method using urea hydrolysis under refluxing conditions. The platelet sizes can be controlled by carefully adjusting the concentrations of metal salts and urea. The as-prepared Co−Al−CO_3 LDH was successfully decarbonated in a NaCl−HCl mixed solution without any morphological change or weight loss. Furthermore, LDHs with a variety

(21) (a) Matsumoto, Y.; Murakami, M.; Shono, T.; Hasegawa, T.; Fukumura, T.; Kawasaki, M.; Ahmet, P.; Chikyow, T.; Koshihara, S.; Koinuma, H. *Science* **2001**, *291*, 854. (b) Ueda, K.; Tabata, H.; Kawai, T. *Appl. Phys. Lett.* **2001**, *79*, 988. (c) Ando, K.; Saito, H.; Jin, Z. W.; Fukumura, T.; Kawasaki, M.; Matsumoto, Y.; Koinuma, H. *Appl. Phys. Lett.* **2001**, *78*, 2700. (d) Fukumura, T.; Yamada, Y.; Tamura, K.; Nakajima, K.; Aoyama, T.; Tsukazaki, A.; Sumiya, M.; Fuke, S.; Segawa, Y.; Chikyow, T.; Hasegawa, T.; Koinuma, H.; Kawasaki, M. *Jpn. J. Appl. Phys.* **2003**, *42*, L105. (e) Bryan, J. D.; Santangelo, S. A.; Keveren, S. C.; Gamelin, D. R. *J. Am. Chem. Soc.* **2005**, *127*, 15568.
(22) Osada, M.; Ebina, Y.; Takada, K.; Sasaki, T. *Adv. Mater.* **2006**, *18*, 295.

of anions (such as NO_3^-, ClO_4^-, acetate, lactate, dodecyl sulfate, and oleate) were prepared from the obtained Cl^--LDH via a normal anion-exchange process. Most of these intercalation products exhibited a delamination behavior in formamide. Among them, NO_3^--LDH was found to have the best delamination behavior. The delamination yielded well-defined nanosheets with a lateral size of micrometer scale. The delamination of LDHs in formamide was revealed to involve two separate stages: rapid swelling into a highly swollen phase, and then progressive exfoliation into single sheets. Multilayer composite films of the exfoliated LDH nanosheets and PSS were assembled in a layer-by-layer fashion. MCD measurements demonstrated that Co−Al LDH nanosheets acted as nanoscale ferromagnetic layers at room temperature, and their multilayer assemblies exhibited significant magneto-optical response in the ultraviolet−visible region.

In addition, the present synthetic method for Co−Al−CO_3 LDH has been extended to other types of transition metal-bearing LDHs (such as Fe−Al, Zn−Al, and Ni−Al), and large-sized platelets of them have been prepared. The availability of large particles of various transition metal-bearing LDHs makes it very promising to obtain their nanosheets. In fact, Ni−Al LDH nanosheets have been produced through a series of procedures as described in the present paper. The related results will be published elsewhere.

Acknowledgment. We are grateful to Prof. Ogawa at Waseda University for his kind discussion on the preparation of Co-Al-CO_3^2-LDH samples. This study was supported by CREST of Japan Science and Technology Agency (JST).

Supporting Information Available: FT-IR spectrum and TG/DTG/DTA curves of the as-prepared Co−Al−CO_3 LDH, SEM images of the Co−Al−CO_3 LDH samples prepared under different conditions, FT-IR spectra, TG curve, and SEM images of the decarbonated and anion-exchanged LDHs, SEM images of the swollen particles before and after being treated with water, XRD pattern of the sample recovered from the swollen phase by treating with water, AFM images of the nanosheets derived from LDHs in different forms, UV−vis absorption spectra of multilayer film of $(LDH/PSS)_n$ measured after every 10 cycles. This material is available free of charge via the Internet at http://pubs.acs.org.

JA0584471